clean technologies

MDPI

Article

Process and Carbon Footprint Analyses of the Allam Cycle Power Plant Integrated with an Air Separation Unit

Dan Fernandes, Song Wang, Qiang Xu, Russel Buss and Daniel Chen *

Dan F. Smith Department of Chemical Engineering, Lamar University, Beaumont, TX 77710, USA; dfernandes@lamar.edu (D.F.); swang5@lamar.edu (S.W.); xuq1@lamar.edu (Q.X.); rabnotes@icloud.com (R.B.)
* Correspondence: daniel.chen@lamar.edu; Tel.: +1-409-880-8786

Received: 15 September 2019; Accepted: 12 October 2019; Published: 15 October 2019

Abstract: The Allam cycle is the latest advancement in power generation technologies with a high cycle efficiency, zero NO_x emission, and carbon dioxide available at pipeline specification for sequestration and utilization. The Allam cycle plant is a semi-closed, direct-fired, oxy-fuel Brayton cycle that uses high pressure supercritical carbon dioxide as a working fluid with sophisticated heat recuperation. This paper conducted process analyses including exergy analysis, sensitivity analysis, air separation unit (ASU) oxygen pump/compressor option analysis, and carbon footprint analysis for the integrated Allam power plant (natural gas)/ASU complex with a high degree of heat and work integration. Earlier works on exergy analysis were done on the Allam cycle and ASU independently. Exergy analysis on the integrated plants helps identify the equipment with the largest loss of thermodynamic efficiency. Sensitivity analysis investigated the effects of important ASU operational parameters along with equipment constraint limits on the downstream Allam cycle. Energy efficiency and carbon footprint are compared among the state-of-the-art fossil-fuel power generation cycles.

Keywords: Allam cycle; air separation unit; carbon capture and utilization; exergy; power generation; oxy-fuel

1. Introduction

The recent report "The Fourth National Climate Assessment" by the US Global Change research program expounds that climate change is real and the global temperature will rise in the future, which will have serious health and economic impacts to the US as well as the rest of the world [1]. The rise in the global emissions of carbon dioxide, approximately 2.7 percent in 2018, will bring fossil fuel production and other industrial emissions to a record high of 37.1 billion tons of carbon dioxide per year. According to the United Nations (UN) backed scientific panel 2018 report, nations have barely a decade left to take extraordinary measures to cut the greenhouse gas emissions in half by the year 2030 so as to keep the Earth's warming below 1.5 degrees Celsius to avoid a global climate change [2]. However, the growth of global economy, especially in developing countries like China and India will swell the energy demand, thereby increasing global emissions of carbon dioxide.

One of the major drivers of energy demand is electricity generation which for the most part, involves the generation of carbon dioxide and other greenhouse gas emissions. For the year 2017, the total world electricity generation was 25,721 TWh out of which coal fired power plants, oil, and natural gas plants generated 16,590 TWh [3] of electricity, with the remaining from other sources. Twenty five percent (25%) of the global CO_2 emissions are from fossil fuel powered plants for electricity and heat production, residential/commercial/public services account for 6%, manufacturing industries

21%, transport 14%, and other sectors 34% [4]. All of these sectors combined lead to the rise in the part per million levels of CO_2 in the atmosphere. The emissions can be both direct which arise during operation of the power plant and indirect which arises during other non-operational phases of the life cycle. The highest carbon dioxide emission is seen in fossil fuel powered plants (coal, oil, and gas). Figure 1a,b show the emission of carbon dioxide from various sources from the US in 2017 and the World in 2014.

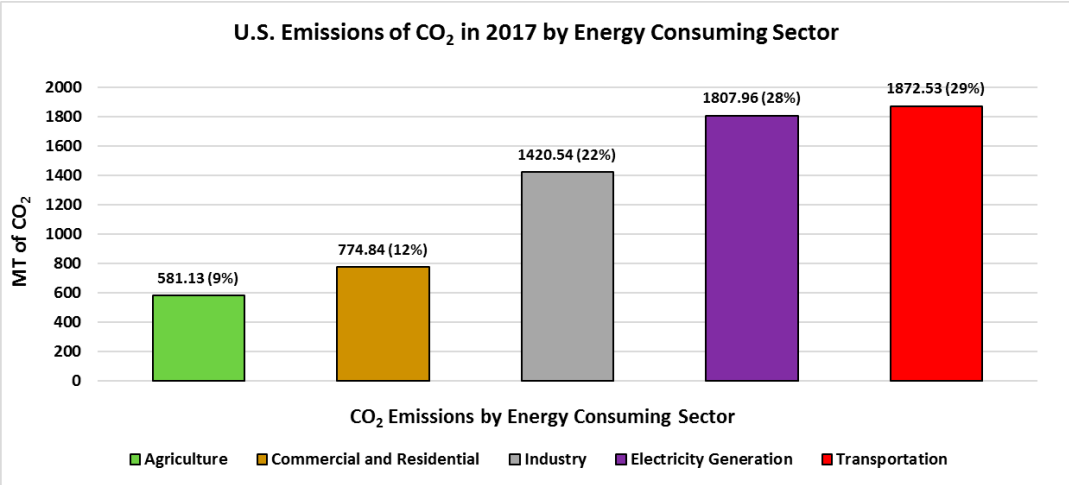

(**a**)

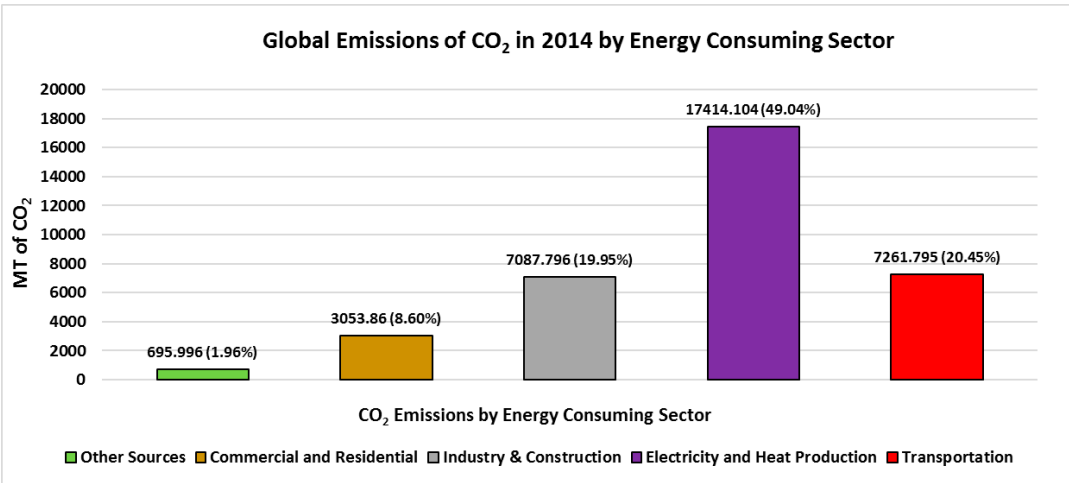

(**b**)

Figure 1. U.S. emissions of CO_2 in 2017 (**a**) and global emissions of CO_2 in 2014 (**b**) by the energy consuming sector [5].

New technological solutions are required so as to mitigate CO_2 emissions from fossil fuel based power generation (for instance, coal accounts for ~60% of electricity production in China). The intermittent nature, land usage, cost issues, and other restrictions make renewable energy technologies like solar, wind, hydro-electric, and biomass systems difficult for worldwide implementation as the base load power sources [6]. The shale gas revolution in the US along with the dramatic increase in the global recoverable natural gas resources and rapid energy usage in the developing world show that fossil fuels will continue to be relied upon in the near future due to its cheaper costs. Therefore, the most likely path to a sustainable energy future is by economically and cleanly employing hydrocarbon energy reserves that can inherently capture combustion derived CO_2 for sequestration or reuse.

There are four types of carbon capture process: post-combustion, pre-combustion, chemical looping, and oxy-fuel supercritical CO_2 cycle. In post combustion processes, the CO_2 separation is done after combustion by an absorption (using amine) or adsorption process. This technology is expensive owing to low capture efficiencies at very low CO_2 concentrations (flue gas containing mostly N_2 and water vapor). In the pre-combustion capture process, coal is gasified in the presence of low oxygen levels to form syngas, which undergoes a water gas shift reaction to form H_2 and CO_2. The separation, however, still incurs a high energy penalty due to sorbent regeneration. The chemical looping combustion process is applied to coal gasification plants. It uses a metal oxide as an oxygen carrier for combustion. During the combustion process the metal oxide is reduced to metal while the fuel undergoes oxidation to produce CO_2 and water. This technology is under development and there is insufficient experience for large scale operation. The last carbon capture technology, the oxy-fuel combustion process with supercritical CO_2 (sCO_2) as the working fluid, can be applied to both coal and gas fired power plants. Here oxygen is used instead of air for the combustion process, eliminating NO_x emissions. This process does incur an energy penalty due to cryogenic O_2 production. The Allam power cycle falls into this category, but the high degree of heat recuperation plus high temperature/high pressure operations are more than enough to overcome the added air separation unit (ASU) load and offer an inexpensive carbon neutral path for a sustainable future [7,8].

In the Allam cycle, Figure 2, a pressurized natural gas reacts with pressurized oxygen from the air separation unit (ASU) in a combustor along with a recycle stream of high pressure/high temperature carbon dioxide. The combustor operates at a pressure of 300 bar and the temperature of the exit combusted gas is 1150 °C. An extremely high combustion temperature results when oxy-fuel combustion is used which requires the use of a diluent like carbon dioxide to lower it to a level that the combustor materials can sustain. The novelty of the design is the use of the supercritical CO_2 working fluid and the higher pressure and temperature. The benefits of using supercritical CO_2 are: (1) the liquid like density which lowers the compression/pumping cost when recycled and requires a smaller size of the turbomachinery, (2) the non-flammable nature, and (3) less corrosion than using steam. The adiabatic flame temperature is the highest temperature attainable and it increases with pressure. The hot gases from the combustor are led into the turbine which is a double shell structure (outer and inner casing) that serves to contain the system's high pressure. The carbon dioxide which is obtained from the lower temperature end of the plant is fed between the space of the inner casing and outer casing to cool it and prevent the metal from reaching its metallurgical limits. This turbine is a hybrid of both the gas technology turbine and steam technology turbine since it operates at the high temperature of the gas turbine and high pressure of the steam turbine. For the Allam cycle, the combustor and the turbine were developed by Toshiba. The exhaust of the turbine is at a pressure of 30 bar and a temperature of 744 °C which feeds to a series of high-pressure multi-channel diffusion bonded recuperative heat exchangers developed by Heatric. It is made up of a high temperature section which cools the gas from 700 °C to 550 °C and another three sections downstream that are used to cool the turbine exhaust to 45 °C by heating the recycled supercritical CO_2 to the combustor. The separator separates the carbon dioxide from water of the exhaust gas stream of the turbine at a pressure of 17 bar and a temperature of 20 °C. Carbon dioxide is compressed in a compressor to a pressure of 100 bar and 97% of it is recycled back to the combustor after being cooled in the cooler to its liquid phase and pumped. Note that at a temperature of 30.98 °C and a pressure of 73.8 bar, the carbon dioxide reaches the critical point. The liquid carbon dioxide is pressurized to 310 bar by a pump and it feeds to the combustor via the recuperator heat exchanger. For the moderation of the adiabatic flame temperature in the combustor, the supercritical carbon dioxide is mixed with oxygen from the ASU to form a mixture at 25 mol% O_2. The remaining 3% of CO_2 produced by the oxy-fuel combustion of natural gas and oxygen must be continuously purged from the process for enhanced oil recovery (EOR)/sequestration and utilization to maintain the mass balance of the system. The amended 45Q (carbon capture and storage tax credit) under the FUTURE act (2018) provides incentive in the form

of tax credit of \$35/ton for CO_2 stored geologically through EOR or \$50/ton for CO_2 stored in other geologic formations and not used in EOR [9].

Imbalances in the thermodynamic properties between the hot gases leaving the turbine and the recycled CO_2, requires a low temperature heat input from the ASU. The cause of the imbalance is due to the difference in the specific heat between the 300 bar recycled CO_2 stream and 30 bar turbine exhaust stream at the low temperature end of the recuperating heat exchanger. The heat input (heated thermal fluid) from the ASU's main air compressor intercooler increases the efficiency of the overall cycle due to the drop of an equivalent fuel energy input, which would have otherwise been required to heat up the recycled CO_2 stream [10–12].

Since the sCO_2 cycle operates at high pressures in most of the equipment it results in a high density working fluid, which leads to a smaller equipment size and smaller plant footprint with a lower capital cost. Compared to the conventional steam Rankine cycle or even the ultra-supercritical steam Rankine cycle, the sCO_2 power cycle has the potential to attain significantly higher cycle efficiency. This will lead to lower greenhouse gas emissions, lower fuel cost, and lower water usage [13].

The cryogenic air separation process, also known as air separation unit (ASU), consumes a large amount of electrical energy [14] because the operation is at extremely low temperatures (−170 to −195 °C) [15]. The double column system is still the best in terms of efficiency and capital cost. According to the patent by Allam et al., the double column system is capable of producing O_2 at the required purity for the combustor, which provides for a lower capital cost expenditure as compared to a three column ASU design. A purity of O_2 at 98% is also enough for this process [16]. The two column design has a lower operating cost and any savings in ASU power within the integrated Allam cycle power plant and ASU will increase the net power output and increase the efficiency of the power plant. In the cryogenic air separation process, the main air compressor is required to deliver the air at a pressure of 5.9 bar to the high pressure column (HPC). The bottom liquid of the HPC, which is rich in oxygen, is fed to the low pressure column (LPC) and the low pressure causes LPC temperature to drop by the Joule-Thomson effect. The LPC is refluxed with liquid nitrogen from the top of the HPC after having been flashed and cooled by the Joule-Thomson effect. The oxygen-rich liquid leaving the bottom of the LPC cools the incoming air to the cryogenic heat exchanger. The liquid coming from the top of the LPC is rich in nitrogen which cools the top liquid of the HPC in the sub-cooled heat exchanger. The oxygen produced is 99.5% pure by mole.

Exergy analysis is usually performed for the detailed study of a power plant efficiency and its possible improvement. The term exergy denotes "technical working capacity" and depends on the reference environment. The choice of the reference environment plays a role in the thermal energy being converted to useful work with a higher efficiency at a lower reference temperature [17]. With exergy analysis, the work potential lost (or entropy gain) and the work still available from a particular equipment are analyzed to give a real measure of the equipment efficiency. The types and magnitudes of wastes and losses along with locations can be revealed to make a better use of an energy resource [18,19]. As a result, exergy analysis is a powerful tool for improving industrial processes and reducing environmental impact. The previous exergy analysis reported by Penkuhn et al. was done only for the Allam cycle [12]. This study conducted detailed second law analysis of the integrated Allam cycle and the air separation unit. Identifying the opportunity of reducing exergy destruction in each of the equipment of the integrated plants can help improve the overall efficiency. Exergy analysis also helps to reduce the carbon footprint of a power plant.

2. Methodology

2.1. Process Modeling Basis

The process simulation is based on a 300 MW thermal Allam cycle plant, which requires 3500 tons of oxygen per day. The integrated power plant/ASU complex is more economical due to the large amount of oxygen required by the Allam cycle, otherwise a nearby large ASU with pipeline infrastructure

needs to be built. Furthermore, there must be other customers for the usage of oxygen to justify the pipeline infrastructure. Another merit of integration is the ease of load changes and rejection of plant disturbances with advanced process controls as done by the authors in a separate study. The power generated from the Allam cycle is capable of powering all the equipment of the ASU with power for export. The simulations of the integrated Allam cycle plant with an air separation unit (ASU) were conducted using ASPEN PLUS V.10.ASPEN plus. The modeled process has a high degree of heat integration along with several recycle streams. The heat integration was the use of air compressor's heat stream from the ASU for heating the recycled CO_2 stream at the lower temperature end of the recuperator and the work integration is the usage of the Allam's power plant turbine to power all the equipment of both the plants.

Exergy analysis is conducted in Aspen plus V.10, which contains the property sets: EXERGYMS, EXERGYML (calculated on mass and molar basis respectively), and EXERGYFL (exergy flow rate) for estimating exergy of material/energy streams, unit operations, and utilities. The chemical exergy had to be calculated manually based on the thermochemical data available in the literature [20]. The process flow sheet is based on a 300 MW thermal Allam cycle plant, which requires 3500 tons of oxygen per day. Two different property packages are used: Peng Robinson for the air separation unit and Soave-Redlich-Kwong for the Allam cycle. The feeds and utilities available at the battery limits are given in Table 1.

Another parallel study conducted in this paper is the parametric (sensitivity) analysis of the Allam cycle integrated with an ASU as opposed to previous studies that focused on the Allam cycle only. The sensitivity analysis tool of ASPEN plus was used for this study. Since the ASU is parasitic by nature, the impact of changing the operating parameters like the distillate to feed ratio on the high pressure column, the reflux ratio of the low pressure column, feed air temperature, and feed air pressure was studied. Recommendations for right operating conditions and improvements are given in the results and conclusion pages respectively.

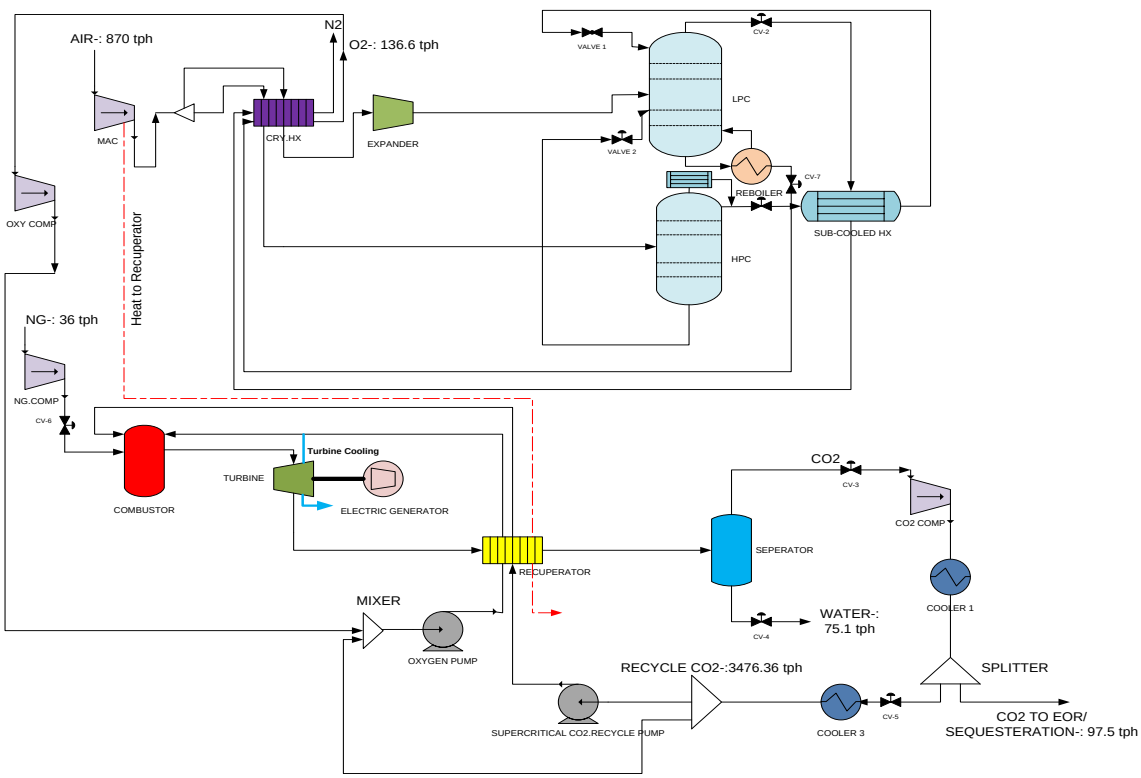

Figure 2. Process flow diagram of the Allam cycle power plant integrated with an air separation unit (ASU) [7,22].

Table 1. Conditions [21] and feedstock compositions [12] at battery limits.

Site Conditions	Air Composition (Mass/Mass)	Natural Gas Composition (Mole/Mole)
Site: Houston, TX	Nitrogen (N_2): 0.7809	Nitrogen (N_2): 0.002
Ambient Pressure: 1.013 bar	Oxygen (O_2): 0.2095	Methane (CH_4): 0.97
Dry Bulb Temperature: 21.89 °C	Argon (Ar): 0.0093	Ethane ($C2H_6$): 0.015
Wet Bulb Temperature: 18.28 °C	Carbon Dioxide (CO_2): 0.003	Propane ($C3H_8$): 0.013
Relative Humidity: 64%	Pressure: 1.013 bar	N-Butane (C_4H_{10}): 0.004
CW Temperature: 15.6 °C	Temperature: 30 °C	Carbon Dioxide (CO_2): 0.010
CW Pressure: 3.0 bar	Flow Rate: 870 tph	Pressure: 30 bar
		Temperature: 38 °C
		LHV: 47457 kJ/kg
		HHV: 52581 kJ/kg
		Flow Rate: 36 tph

2.2. Air Separation Unit Modeling

The Peng-Robison equation of state is the thermodynamic method used for the ASU to describe the vapor-liquid and liquid-liquid equilibria. It is also useful to predict liquid densities of non-polar gases (O_2 and N_2) used in modeling cryogenic air separation units [23].

The modeling parameters for the high pressure column (HPC) and low pressure column (LPC) are given in Table 2. The number of stages were initially calculated based on the DSTWU method using the Winn-Underwood-Gilliland method. Then a detailed column design was done using RadFrac column. Dynamic simulation of the column determined the optimum number of stages for the required separation and purity of O_2 desired including consideration for flooding and weeping of the column and sieve tray specification selection. This design was then validated with the work of Raibhole et al. [23]. The oxygen specific power, the most important performance indicator of the ASU, is defined as the total power consumption per normal cubic meter of oxygen produced. It is 0.55 kW/scmh of oxygen in this simulation. The high purity oxygen plants operate at low thermodynamic efficiency with its oxygen specific power in the range of 0.5–0.6 kW/scmh.

Table 2. Summary of design parameters of high pressure column (HPC) and low pressure column (LPC) [23].

Column Parameters	HPC	LPC
Number of Stages	39	55
Feed Temperature (°C)	−178	−192
Reflux Ratio	0.196	0.72
Condenser Temperature (°C)	−176	−192.8
Condenser Pressure (bar)	5.8	1.2
Distillate Rate (kmol/h)	22179.5	25891.8
Reboiler Temperature (°C)	−173.35	−181.5
Bottom Rate (kmol/h)	4961.34	4264.65

2.3. Allam Cycle Modeling

The combustor is one of the most important components of a gas turbine plant. The power output of the turbine is proportional to the temperature of the gases produced in the combustor [24]. For a stoichiometric air-fuel mixture under adiabatic conditions the highest temperature obtained is called the adiabatic flame temperature [25]. The combustor is modeled as an RGibbs reactor as the high temperatures justify the assumption of chemical equilibrium. The turbine is modeled according to the work of Scaccabarozzi et al. [26] which considers the three stage turbine cooling method. The isentropic efficiency of the turbine is linearly proportional to the net electric efficiency of the cycle. Increasing the isentropic efficiency of the turbine with one percentage point causes the overall electric efficiency to increase by 0.33 percentage points. In this study the isentropic efficiency was taken as 93%. The exhaust of the turbine going to the recuperator is made up of three sections (a hot temperature

section, an intermediate temperature section, and a low temperature section) to avoid temperature cross over effects [27,28]. Incomplete combustion is taken into account even though the formation of carbon monoxide and soot is negligible due to the extreme high combustor temperature and pressure.

The thermodynamic package used is Soave-Redlich-Kwong (SRK) for the Allam cycle even though Peng-Robinson is also appropriate. The reason for choosing SRK is this equation of state (EOS) agrees with the experimental density data of the CO_2-O_2 binary mixture with a relative error of 2.2% [26]. The centrifugal compressors are modeled with a polytropic efficiency of 80% to account for the change in the characteristics of the gas during compression and a mechanical efficiency of 98% [29]. The pumps have an efficiency of 75%. The net power for export is 284 MW and the efficiency of the plant is 59.8% with the net specific work from the plant being 307 kJ/kg of natural gas. Higher net specific work with increased plant efficiency will be obtained if the ASU pumps oxygen instead of compressing it. Table 3 highlights the comparison between the plant performance characteristics of the simulation of air separation unit in which oxygen is a gas and is compressed by a compressor to an air separation unit in which oxygen is a liquid and is pumped.

Table 3. Comparison of simulated plant performance parameters with oxygen compressor and oxygen pump.

Plant Performance Parameters	ASU with O_2 Compressor	ASU with O_2 Pump
Net Electric Power Output (MW)	284	305.4
Plant Thermal Efficiency (%)	59.8	64.3
Net Specific Work (kJ/kg)	307	330.5
Power Consumption in ASU (MW)	71.3	52.2
ASU Specific Power Demand (kW/scmh)	0.5	0.4
Pump/Comp. Power Consumption (MW)	19.5	0.4

In the work conducted by Mitchell et al. [30] the net cycle efficiency can increase to 66.10% when the Allam cycle plant is run on stored oxygen, increasing the net electric output by 17.67%, through the avoidance of oxygen production penalty.

2.4. Exergy Analysis for the Integrated Plants

Exergy is the maximum work that can be obtained from a system during a process that brings this system into equilibrium with its surroundings (at a reference state characterized by a temperature T_0 and a pressure P_0). The exergy of the system will be zero once the system and its surroundings reach equilibrium [31]. The energy balance is not suitable to identify the real loss in quality of energy because the law of conservation of energy will always apply, whereas in an exergy balance it gives the real loss in the quality of energy [32]. Since real process are irreversible, the total exergy flowing into any unit operation is greater than the total exergy flowing out, some exergy is lost during the unit operation. Ahrendts [33] suggested to use 25 °C and 1.013 bar as the standard or reference state for chemical exergy for an environment in equilibrium. One effect of this choice is a lower chemical exergy for gaseous and liquid water, the latter being very small.

In this work, the EXERGYFL from the ASPEN simulation was used. Exergy transfer has several modes namely work and heat exergy, material stream exergy, and exergy destruction. The other components of exergy transfer, such as potential and kinetic exergies are neglected.

The mode of exergy transfer with work is given as:

$$E_{work} = W, \tag{1}$$

where, E_{work} is the exergy transferred due to work interaction and W is work. In ASPEN PLUS, work is (+) when added to the equipment and negative (–) when it is generated. In the mode of exergy heat flow:

$$E_{heat} = Q\left(1 - \frac{T_0}{T}\right), \tag{2}$$

where, E_{heat} is the exergy transfer due to heat interaction, Q is the heat transfer rate, T_0 and T is the ambient temperature and temperature at which heat transfer take place respectively.

The exergy of the material stream is split into its chemical and physical parts for the analysis of the power cycle [34], E_{Ch} and E_{Ph} is the exergy due to the chemical and physical components, respectively.

$$E_m = E_{Ch} + E_{Ph} \tag{3}$$

The physical exergy is the work obtainable by taking the substance through reversible processes from its initial state temperature T and pressure P, to the environmental state given as T_0 and P_0 at which the free enthalpy and entropy of formation are calculated [35].

$$E_{Ph} = H - H_0 - T_0(S - S_0), \tag{4}$$

where, H is the enthalpy and S is the entropy.

The chemical exergy is equal to the maximum amount of work obtainable when the substance under consideration is brought from the environmental state, defined by the parameters T and P to the standard dead state by the process involving heat transfer and exchange of substances only with the environment.

$$E_{Ch} = \sum x_i[e_{0i} + RT_0 \ln(\gamma_i x_i)], \tag{5}$$

where, x_i is the molar fraction of the component i and e_{0i} is the standard chemical exergy obtained from thermodynamic tables given in kJ/mol. Here γ_i is the activity coefficient of the component i which is taken to be 1.

The exergy destruction also called irreversibility or exergy loss is given as:

$$E_{destruction} = E_{min} - E_{mout} + E_{work} + E_{heat}, \tag{6}$$

where, E_{min} and E_{mout} is the flow of the material exergy streams in and out respectively.

The simple exergy efficiency of the ith component is given by:

$$\eta_{exergy,i} = 1 - \frac{E_{\text{destruction}}}{E_{in}}, \tag{7}$$

where, E_{in} is the $E_{min} + E_{heat} + E_{work}$,

This is used for most of the equipment. However, for a heat exchanger, pump, compressor and distillation column, the rational exergy efficiency is used. It is the ratio of the desired exergy output to the exergy used for that purpose. For the heat exchanger it is given by:

$$\Psi = \frac{\sum_G \Delta E_G}{\sum_L \Delta E_L}, \tag{8}$$

where, ΔE_G is the thermal component gained by the Gth stream and ΔE_L is the thermal component lost by the Lth stream.

For a distillation column, the rational exergy is described by Equation (9). For a pump and a compressor, the rational exergy efficiency is given by Equation (10).

$$\Psi = \frac{W_{min}}{W_{min} + \Delta E_{loss}}, \tag{9}$$

$$\Psi = \frac{E_{in} - E_{out}}{W_{in}}, \tag{10}$$

where W_{min} is the minimum work of separation, ΔE_{loss} is the exergy lost by the column, W_{in} is the total power input in kW, E_{in} is the exergy in, and E_{out} is the exergy out in kW [36].

2.5. Carbon Footprint Analysis

The exergy analysis done in the previous section helps to determine the environmental impact (carbon footprint) of the integrated Allam/ASU power plant. Even though in the Allam cycle the carbon footprint is taken to be zero, since it is used for EOR/feedstock/sequestration, improving its efficiency by identifying the equipment of high exergy destruction can reduce the amount of CO_2 generated in case sequestration is the only feasible means of disposal.

A 'carbon footprint' is the total amount of CO_2 and other greenhouse gases, emitted over the full life cycle of a process or product. It is expressed as grams of CO_2 equivalent per kilowatt hour of generation (gCO_2/kWh). For fossil fueled power plants, the carbon footprint is by the CO_2 emissions during the operational period of the plant. The indirect emissions during other life cycle phases like plant construction and mining of raw material is minor. Increasing the net power output of the power plant with the lower consumption of fuel, by identifying and improving the efficiency of each individual equipment will reduce the carbon footprint [37].

3. Results and Discussion

3.1. Exergy Analysis

3.1.1. Exergy Analysis Results of the Air Separation Unit (ASU)

In the exergy analysis of the ASU, the highest destruction of exergy is seen in the cryogenic heat exchanger (60.82%), the main air compressor (16.39%), and the oxygen compressor (7.48%). Figure 3 shows the chart of exergy destruction.

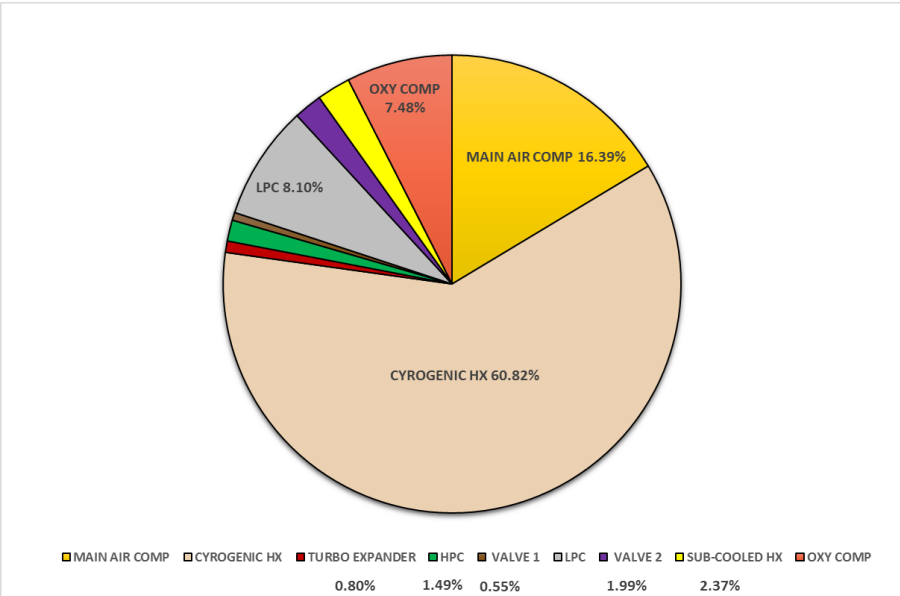

Figure 3. Air separation unit exergy destruction chart.

The possible causes of high destruction in the cryogenic heat exchanger are due to the cooling of the air by exchanging heat with the N_2 and O_2 streams from the LPC. The probable exergy destruction for the main air compressor is due to the thermal input to the lower end of the recuperator in the Allam power plant. Table 4 shows the comparison of the exergy efficiency of this work for an ASU/ Allam power cycle complex and the work done by Sapali et al. [36] for a standalone ASU.

Table 4. Exergy efficiency of the air separation unit.

Component	Exergy Efficiency (%)	Exergy Efficiency (%)
	This Work	Sapali et al., 2013
Main Air Compressor	70.6	64.4
Cryogenic Heat Exchanger	57.7	56.4
Turbo Expander	59.9	50.2
High Pressure Column	44.9	50.2
Joule Thompson Valve 1	98.0	NA
Low Pressure Column	79.8	54.0
Joule Thompson Valve 2	98.4	NA
Sub-Cooled Heat Exchanger	69.1	88.2
Oxygen Compressor	65.6	NA

3.1.2. Exergy Analysis Results of the Allam Cycle

In the Allam cycle, the highest exergy destruction is seen in the combustor which is at 31.37%, then followed by the recuperator at 28.68%, and the turbine at 23.62%. Figure 4 gives the detailed chart of exergy destruction of the Allam cycle components and Table 5 shows the comparison of the Allam cycle exergy efficiency of this work with the work done by Penkuhn et al. [12]. The minor differences between the two studies can be attributed to: (1) a detailed ASU model was used in this work while a simple black box model was used for the ASU in Penkuhn et al.'s work and (2) the ambient condition chosen is 25 °C in our work (location Houston) and 15 °C in the work of Penkuhn et al. (location Midwest). This choice of reference temperature affects the component molar exergies and the chemical exergy of the given equipment.

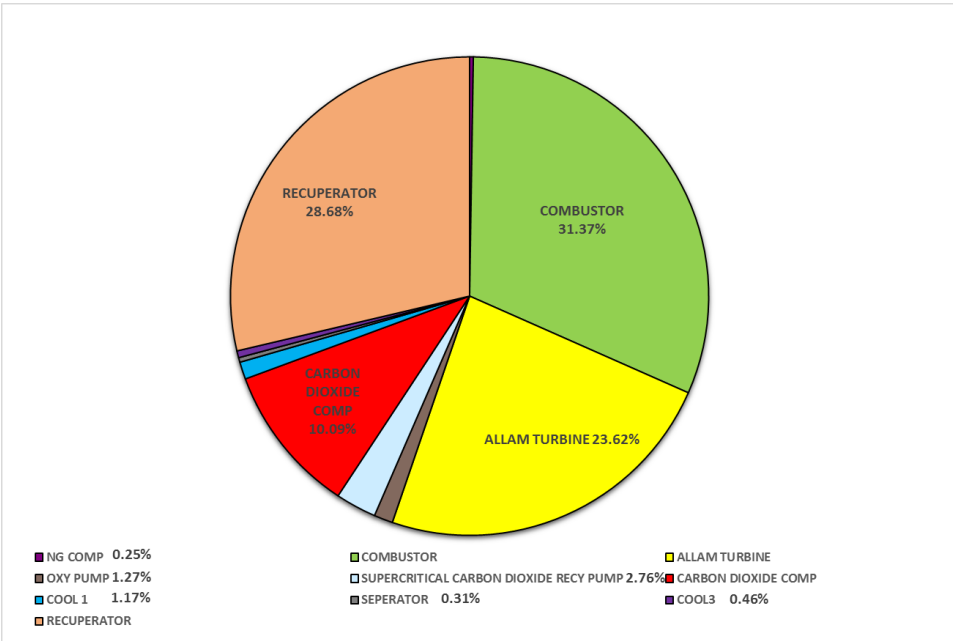

Figure 4. Allam cycle exergy destruction chart.

Possible cause of the exergy destruction in the recuperator is due to the exchange of heat between the recycled sCO_2 stream and the turbine exhaust. The loss of the exergetic efficiency in the Allam turbine could also be due to the cooling of the turbine blades by the sCO_2 coolant.

The temperature-entropy (T-S) plot shown in Figure 5 illustrates various stages of the Allam power cycle. Point A is the turbine inlet and Point B is the turbine outlet. The cooling of the turbine exhaust by the exchange of the heat with the recycled CO_2 takes places from Point B to Point C (Line BC) in

the recuperator. Line CD represents the cooling of CO_2 and separation of water from the exhaust stream. Point D is the CO_2 compressor suction and its compression with intercooling is abbreviated as Line DE. In Line EF the recycled CO_2 is further cooled in the aftercooler, which results in an increase in density. From Point F to Point G the recycle pump increases the pressure of the recycled CO_2 to 312 bar. From Point G to Point H, the recycled CO_2 exchanges heat with the exhaust of the turbine in the recuperator. The combustion process takes place from Point H to Point A. Figure 5 illustrates how the thermodynamic variables (temperature and entropy) change during the Allam cycle unit operations (combustion, expansion, heating/cooling, compression, pumping, etc.) and is particularly relevant from the exergy analysis point of view.

Table 5. Exergy efficiency of the Allam cycle.

Component	Exergy Efficiency (%)	Exergy Efficiency (%)
	This Work	**Penkuhn et al., 2016**
Natural Gas Compressor	89.7	85.7
Combustor	95.2	78.3
Allam Turbine	91.0	92.8
Oxygen Pump	71.3	50.1
Supercritical CO_2 Pump	74.7	68.2
CO_2 Compressor	60.9	85.5
Cooler 1	23.3	NA
Separator	99.5	89.6
Cooler 3	14.0	22.2
Recuperator	86.3	96.8

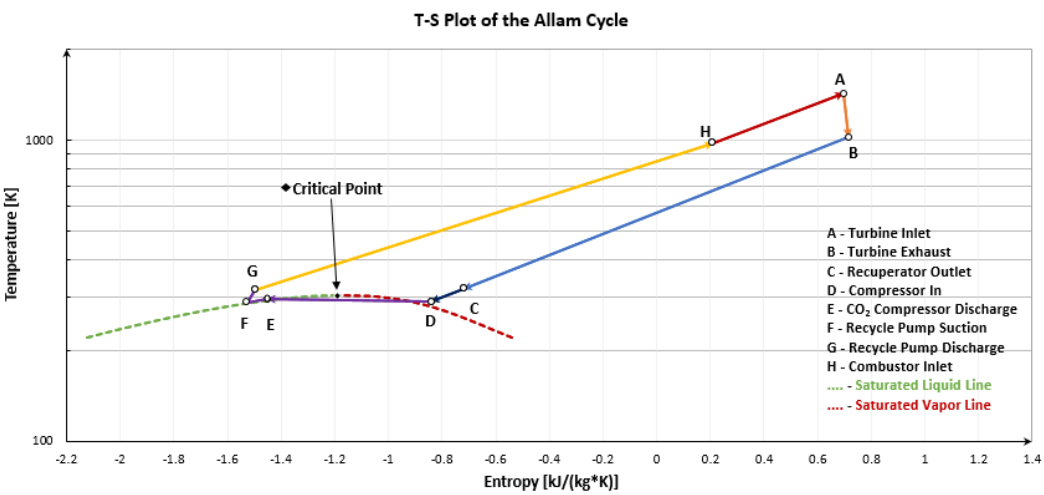

Figure 5. Temperature-entropy plot of the Allam power cycle.

3.2. Sensitivity Analysis of the ASU Operating Parameters on the Allam Power Cycle

This section analyzes the influence of the operating parameters (including disturbances) of the air separation unit on the Allam power cycle. The following operating parameters are varied and its effects on the Allam cycle are studied:

- distillate to feed ratio of the high pressure column;
- reflux ratio of the low pressure column;
- ambient air temperature; and
- ambient air pressure.

The observed effects on the Allam cycle plant include, the purity of piped carbon dioxide in mole fraction, the turbine outlet temperature in degrees Celsius and net power for export. The purity of

piped carbon dioxide is important because water, if present, can lead to corrosion problems in the pipeline. Turbine outlet temperature is another important parameter to monitor because of the material limitations of the recuperator downstream of the turbine.

3.2.1. Effect of Varying the Distillate to Feed Ratio in the High Pressure Column (HPC)

Here the distillate to feed ratio (D/F) of the high pressure column is varied between 0.81 and 0.82 using the sensitivity analysis tool of ASPEN PLUS while keeping all other parameters constant. Figure 6 shows the effect of varying the distillate to feed ratio of the high pressure column. As can be seen, the best CO_2 purity (97.7%) is at 0.8172 (D/F). Operation at any lower/higher ratio will reduce the purity of piped CO_2 stream. If a high purity CO_2 stream is required for a feedstock, like a urea plant integrated with the power plant, this can be a cause for concern if the operating parameter varies from this value. It is thus recommended to install a carbon dioxide processing unit for the piped CO_2 stream to handle a deviation from this operating point. The turbine exhaust temperature are also within the limits of its operating range.

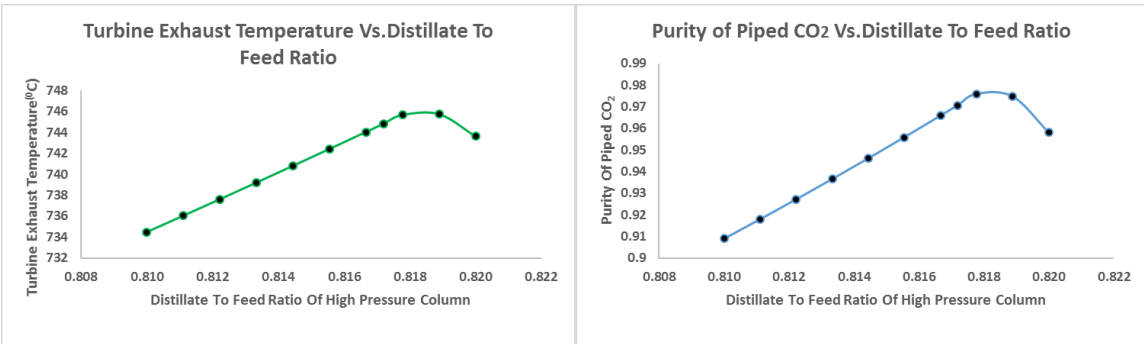

Figure 6. Effect of varying the distillate to feed ratio of the high pressure column.

3.2.2. Effect of Varying the Reflux Ratio of the Low Pressure Column (LPC)

In this scenario, the reflux ratio (RR) is varied between 0.7 and 0.72. The purity of piped CO_2 (89%) is lower at 0.7 RR. The turbine outlet temperature is around 760 °C, which is much higher than the temperature (750 °C) that the Heatric heat exchanger (made of Inconel 617 alloy) can tolerate. Figure 7 shows the effect of varying the reflux ratio of the LPC. For this simulation the RR of 0.72 was chosen so that the turbine exhaust temperature will remain at 744 °C. If the RR drops due to an operator error or some unforeseen disturbance in the ASU unit, it is recommended that the recycled CO_2 stream to the combustor be increased to reduce the turbine exhaust temperature and the load of the plant should be dropped. The purity of piped CO_2 is the highest at 0.72.

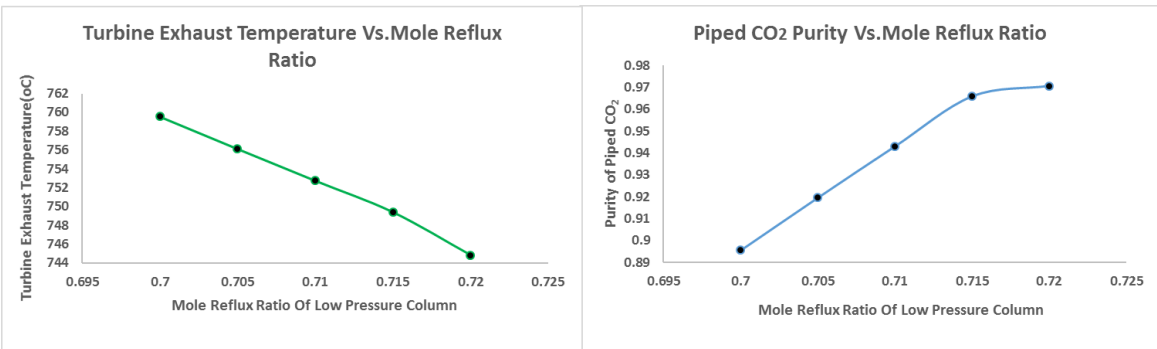

Figure 7. Effect of varying reflux ratio of the low pressure column.

3.2.3. Effect of the Ambient Air Temperature and Pressure to the ASU Power Demand

The ambient air temperature ranges between −2 and 40 °C, which is experienced in Houston, Texas during the winter and summer, respectively. The power requirements of the main air compressor increase as the ambient temperature increases as shown in Figure 8. For the ambient pressure, comparison was done between Houston, Texas, which is located at the sea level and Denver, Colorado, which is located at an elevation of 5280 feet (1609 m). In this case, the power requirement for the main air compressor is more for the lower barometric pressure location (Denver) and less for the higher barometric pressure location (Houston) as shown in Figure 9. Therefore, low elevation with a high ambient pressure should be favored.

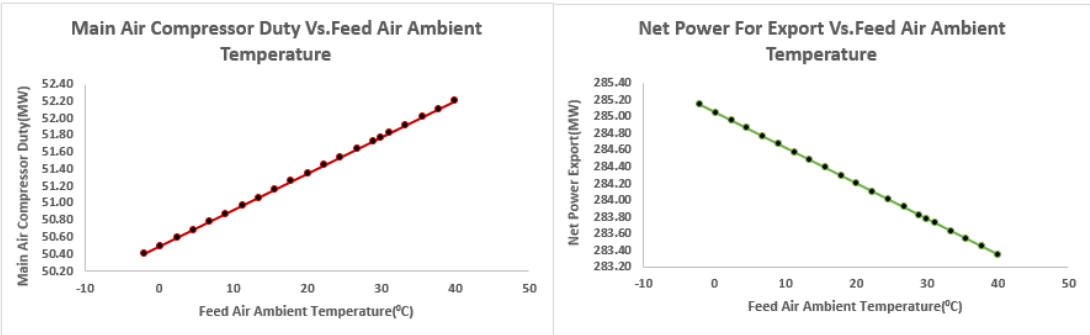

Figure 8. Effect of the disturbance in ambient air temperature on the Allam cycle performance.

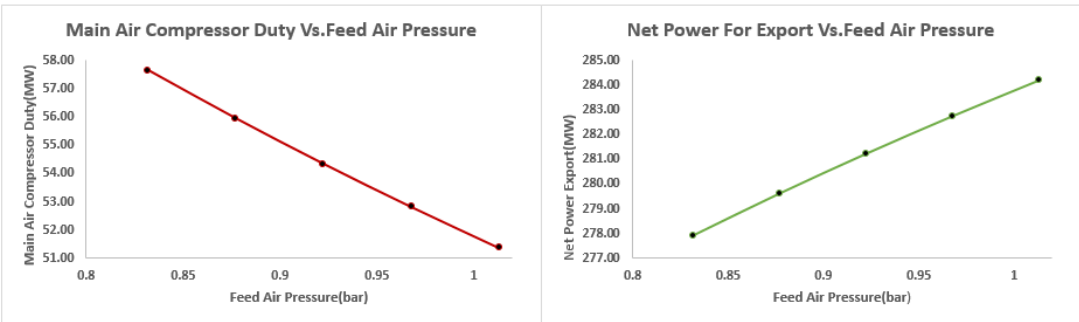

Figure 9. Effect of the disturbance in ambient air pressure on the Allam cycle performance.

3.3. Carbon Footprint Comparison and Impact on Global Carbon Dioxide Emission Levels

Table 6 shows the carbon footprint comparison between an Integrated Gasification Combined Cycle (IGCC) power plant with and without carbon capture, a Natural Gas Combined Cycle (NGCC) power plant with and without carbon capture, an Indirect-fired sCO_2 Recompression Brayton cycle power plant, and an Allam cycle (Direct-fired Oxy-fuel sCO_2 Brayton cycle) power plant. In general, there is an efficiency penalty associated with carbon capture except for the Allam cycle for which the generated CO_2 is sent at the pipeline grade specification for EOR/utilization/sequestration. It can be seen that the high thermal efficiency of the Allam cycle power plant (59.8%) is achieved even with the requirement of an associated air separation unit.

Based on the Table 6 results and the following assumptions: (1) all power plants are converted to the Allam cycle; (2) all generated pipeline-grade CO_2 can be sequestered or utilized (3) power generation by renewable energy sources are not considered; (4) all other carbon emissions remain constant; (5) the global power generation carbon footprint is constant at 49.04% as shown in Figure 1b; (6) all earth source/sink dynamics remain the same; and (7) 1 Gt of CO_2 emission = 0.127 ppm of CO_2 in earth atmosphere, the authors performed the following simplistic calculations to estimate the potential benefit of the Allam cycle technology on reducing the global atmospheric CO_2 levels:

Carbon print reduction: from 34.22 Gt/yr to 22.95 Gt/yr
Years to reach 450 ppm level: (450 − 409.36) ppm/[(22.95 Gt/yr) × (0.127 ppm/Gt)] = 13.9 yr
Years to reach 450 ppm level: (450 − 409.36) ppm/[(34.22 Gt/yr) × (0.127 ppm/Gt)] = 9.4 yr

Where 409.36 ppm is the CO_2 level in 2018 and 34.22 Gt/yr is the latest global CO_2 emissions (Baseline). It can be seen the Allam cycle technology alone can potentially delay the time to reach 450 ppm CO_2 (or 2 °C temperature rise) by 4.5 years.

Table 6. Carbon footprint comparison of various power cycles [13,18,38–40].

Comparison Indicators	IGCC *		NGCC *		Recompression sCO_2 Brayton Cycle	Allam Cycle
	With CC *	Without CC *	With CC *	Without CC *	Without CC	
Thermal Efficiency (%)	38.6	44.2	47.7	53.8 ***	52.1	59.8
Carbon Capture (%)	90.1	0	90.7	0	0	100
Carbon Footprint (gCO_2/kWh)	109.7	968	39	373	385.3	0 **
Cycle	Brayton + Rankine				Brayton	Brayton

*: IGCC—Integrated Gasification Combined Cycle. NGCC—Natural Gas Combined Cycle. CC—Carbon Capture (Post Combustion). **: Under the assumption that piped CO_2 is utilized for enhanced oil recovery (EOR) or chemical feedstock and there are no leaks to the environment. ***: New General Electric HA class turbines have an efficiency of greater than 62%. However, the cost of post combustion capture is expensive.

4. Conclusions and Recommendations

This paper presents a detailed model of the Allam cycle combined with an air separation unit (ASU) with a high degree of heat and work integration. The authors recommend that two plants should be operated by the same company and the power output of the power plant should power the ASU's equipment, rather than depend upon an external grid. This type of arrangement can help reject any disturbances to the operation of the integrated plants quickly and smoothen the operations. Locating the Allam cycle and ASU near coastal areas where the ambient conditions are suitable for peak performance is one important consideration.

Earlier works on exergy analysis were done on the Allam cycle and ASU independently. To the authors best knowledge this is the first exergy analysis work on the integrated plants. It was found that for the ASU, the cryogenic heat exchanger was the major source of exergy destruction followed by the main air compressor. For the Allam cycle, the major exergy destruction was seen in the combustor followed by the recuperator. Comparison of the Allam cycle performance was made between ASU with O_2 compressor and ASU with O_2 pump, it was found that ASU with O_2 pump was more efficient because of a higher net specific work and a lower power consumption. Wide changes in the ASU operating parameters can affect the purity of CO_2 and it is recommended to install a carbon dioxide processing unit to maintain the purity of piped CO_2.

State-of-the-art fossil-fuel power cycles: Integrated Gasification Combined Cycle (IGCC), Natural Gas Combined Cycle (NGCC), and Recompression Supercritical CO_2 Brayton Cycle with the post-combustion carbon capturing technology can only remove approximately 90% of the produced CO_2. On the other hand, the carbon footprint for the Allam cycle is virtually zero because the process produces high pressure, pipeline grade CO_2 that can be utilized for enhanced oil recovery (EOR), as a chemical feedstock, or for underground storage. For a 300 MW Allam power plant, the total CO_2 for EOR/utilization/sequestration per year is 772,200 tons (97.5 tph × 24 hrs × 330 days) if it operates at 330 days per year. If used for EOR, the plant can earn $27 million in 45Q tax credits while if it is used for sequestration in other geologic formation, the tax credit for the plant can be $38.6 million (in the US). It is to be noted that the adoption of the natural gas Allam cycle technology is more effective in reducing global carbon emissions than converting coal-fired power plants to natural gas integrated combined cycle plants with carbon capture.

Further work, using the techniques in this paper, can be conducted to investigate the exergy analysis of the modified Allam Cycle (Z-cycle) proposed by Zhu et al. [41] where they have utilized

high pressure pumps instead of compressors. This would improve upon their findings of efficiency or help in the validation of their work.

Author Contributions: D.F.: Methodology; S.W.: Validation; D.F. and S.W.: Writing—Draft; Q.X.: Writing—review and editing; R.B.: Conceptualization; D.C.: Supervision and Funding Acquisition.

Funding: This research was funded by the Texas Air Research Center (TARC Grant Number: 079LUB0096A and 117LUB0165A) and Lamar University Visionary Initiatives Program (Grant #420065).

Acknowledgments: The authors wish to thank the help of Timothy Meckel of the University of Texas at Austin and Jeffrey Hayes of Port Arthur Chamber of Commerce in the completion of this work.

Conflicts of Interest: The authors declare no conflict of interest.

References

1. USA Global Change Research Program. *Fourth National Climate Assessment. Impacts, Risks and Adaptation in the United States*; USA Global Change Research Program: Washington, DC, USA, 2018; Volume 2.
2. The Intergovernmental Panel on Climate Change. *Global Warming of 1.5 °C*; Special Report; The Intergovernmental Panel on Climate Change: Geneva, Switzerland, 2018.
3. International Energy Agency. *World Energy Statistics, Database Documentation*; International Energy Agency: Paris, France, 2019.
4. The Intergovernmental Panel on Climate Change. *Climate Change: Mitigation of Climate Change*; AR 15 Contribution to the Fifth Assessment Report; The Intergovernmental Panel on Climate Change: Geneva, Switzerland, 2014.
5. Sources of Greenhouse Gas Emissions. Greenhouse Gas Emission. Available online: https://www.epa.gov (accessed on 23 May 2019).
6. Brown, A.; Dobrotova, Z. *Renewable Energy: Markets and Prospects by Technology*; International Energy Agency: Paris, France, 2011.
7. Allam, R.; Palmer, M.; Brown, G.W., Jr.; Glenn, W. System and Method for High Efficiency Power Generation Using a Carbon Dioxide Circulating Working Fluid. U.S. Patent 8,596,075, 3 December 2013.
8. Leung, D.Y.C.; Caramanna, G.; Maroto-Valer, M.M. An overview of current status of carbon dioxide capture and storage technologies. *Renew. Sustain. Energy Rev.* **2014**, *39*, 426–443. [CrossRef]
9. Great Plains Institute. Before and after: How the FUTURE Act Reformed the 45Q Carbon Capture and Storage Tax Credit. 5 March 2018. Available online: https://www.betterenergy.org (accessed on 10 May 2019).
10. Allam, R.; Martin, S.; Forrest, B.; Fetvedt, J.; Lu, X.; Freed, D.; Brown, G.W., Jr.; Sasaki, T.; Itoh, M.; Manning, J. Demonstration of the Allam Cycle: An update on the development status of a high efficiency supercritical carbon dioxide power process employing full carbon capture. *Energy Procedia* **2017**, *114*, 5948–5966. [CrossRef]
11. Isles, J. Gearing up for a new supercritical CO_2 power cycle system. *Gas Turbine World.* **2014**, *44*, 14–18.
12. Penkuhn, M.; Tsatsaronis, G. Exergy Analysis of the Allam Cycle. In Proceedings of the 5th International Symposium-Supercritical CO2 power cycles, San Antonio, TX, USA, 28–31 March 2016.
13. U.S. Department of Energy. *Quadrennial Technology Review. Supercritical Carbon Dioxide Brayton Cycle, Technology Assessments*; U.S. Department of Energy: Washington, DC, USA, 2015; Chapter 4.
14. Xu, Z.; Zhao, J.; Chen, X.; Shao, Z.; Qian, J.; Zhu, L.; Zhou, Z.; Qin, H. Automatic load change system of cryogenic air separation process. *Sep. Purif. Technol.* **2011**, *81*, 451–465. [CrossRef]
15. Huang, R.; Zavala, V.M.; Biegler, L.T. Advanced step nonlinear model predictive control for air separation units. *J. Process Control* **2009**, *19*, 678–685. [CrossRef]
16. Allam, R.J. Cryogenic Air Separation Method for Producing Oxygen at High Pressures. U.S. Patent 2018/0073804, 15 March 2018.
17. Ertesvag, I.S. Sensitivity of chemical exergy for atmospheric gases and gaseous fuels to variations in ambient conditions. *Energy Convers. Manag.* **2007**, *48*, 1983–1995. [CrossRef]
18. Araujo, A.B.; Vasconcelos, R.P. Exergetic analysis of distillation processes—A case study. *Energy* **2012**, *32*, 392–399. [CrossRef]
19. Olaleye, A.K.; Wang, M.; Kelsall, G. Steady State Simulation and Exergy Analysis of Supercritical Coal-fired Power Plant with CO_2 capture. *Fuel* **2015**, *151*, 57–72. [CrossRef]

20. Kaushik, S.C.; Reddy, S.V.; Tyagi, S.K. Energy and exergy analysis of thermal power plants: A review. *Renew. Sustain. Energy Rev.* **2011**, *15*, 1857–1872. [CrossRef]
21. National Oceanic and Atmospheric Administration (NOAA). *Local Climatological Data Annual Summary with Comparative Data*; KIAH: Houston, TX, USA, 2016. Available online: https://www.weather.gov (accessed on 15 May 2019).
22. Raibhole, V.N.; Sapali, S.N. Simulation and Parametric Analysis of Cryogenic Oxygen Plant for Biomass Gasification. *Mech. Eng. Res.* **2012**, *2*, 97–107. [CrossRef]
23. Li, M.L.; Lee, H.Y.; Lee, M.W.; Chien, I.L. *Simulation and Formula Regression of an Air Separation Unit in China Steel Corporation*; ADCONP: Sandton, South Africa, 2014; pp. 213–218.
24. Singh, O.K. Combustion simulation and emission control in natural gas fueled combustor of gas turbine. *J. Therm. Anal. Calorim.* **2016**, *125*, 949–957. [CrossRef]
25. Nag, P.K. *Power Plant Engineering*; McGraw-Hill: New York, NY, USA, 2007.
26. Scaccabarozzi, R.; Gatti, M.; Martelli, E. Thermodynamic analysis and numerical optimization of the NET Power oxy-combustion cycle. *Appl. Energy* **2016**, *178*, 505–526. [CrossRef]
27. White, C.; Weiland, N. Preliminary cost and performance results for a natural gas fired direct sCO2 power plant. In Proceedings of the 6th International Supercritical CO2 Power Cycles Symposium, Pittsburgh, PA, USA, 27–29 March 2018.
28. Allam, R.; Palmer, M.; Brown, G.W., Jr.; Fetvedt, J.; Freed, D.; Nomoto, H.; Itoh, M.; Okita, N.; Jones, C., Jr. High efficiency and low cost of electricity generation from fossil fuels while eliminating atmospheric emissions, including carbon dioxide. *Energy Procedia* **2013**, *37*, 1135–1149. [CrossRef]
29. Larralde, E. *Selection of Gas Compressors: Part 1*; Elsevier: Amsterdam, The Netherlands, 2011.
30. Mitchell, C.; Avagyan, V.; Chalmers, H.; Lcuquiaud, M. An initial assessment of the value of the Allam Cycle power plants with liquid oxygen storage in future GB electricity system. *Int. J. Greenh. Gas Control* **2019**, *87*, 1–18. [CrossRef]
31. Kotas, T.J. *The Exergy Method of Thermal Plant Analysis*, 2nd ed.; Krieger Publishing Company: Malabar, FL, USA, 1995.
32. Tsatsaronis, G. Thermoeconomic analysis and optimization of energy systems. *Prog. Energy Combust. Sci.* **1993**, *19*, 227–257. [CrossRef]
33. Ahrendts, J. Reference States. *Energy* **1980**, *5*, 667–677. [CrossRef]
34. Tsatsarnois, G. Definitions and nomenclature in exergy analysis and exergoeconomics. *Energy* **2007**, *32*, 249–253. [CrossRef]
35. Van der Ham, L.V.; Kjelstrup, S. Exergy analysis of two cryogenic air separation processes. *Energy* **2010**, *35*, 4731–4739. [CrossRef]
36. Sapali, S.N.; Raibhole, V.N. Exergy Analysis of Cryogenic Air Separation Unit Integrated with Biomass Gasifier. In Proceedings of the World Congress on Engineering and Computer Science WCECS, San Francisco, CA, USA, 23–25 October 2013; Volume 2.
37. Carbon Footprint of Electricity Generation Parliamentary Office of Science and Technology. Number 268. October 2006. Available online: https://www.parliament.uk/post (accessed on 20 May 2019).
38. White, C.; Weiland, N.; Shelton, W.; Gray, D. Preliminary Baseline for Direct Fired sCO2 cycles. In Proceedings of the 5th International Supercritical CO2 Power Cycles Symposium, San Antonio, TX, USA, 29–31 March 2016.
39. CB & I/Stone & Webster, Inc. *Assessment of Natural Gas Combined Cycle Plants for Carbon Dioxide Capture and Storage in a Gas Dominated Electricity Market*; Final Project Report; CB & I/Stone & Webster, Inc.: Stoughton, MA, USA, 2014.
40. National Energy Technology Laboratory. *Life Cycle Analysis: Integrated Gasification Combined Cycle (IGCC) Power Plant*; DOE/NETL-403/110209; National Energy Technology Laboratory: Pittsburgh, PA, USA, 2010.
41. Zhu, A.; Chen, Y.; Wu, J.; Zhang, S.; Zheng, S. A modified Allam Cycle without compressors realizing efficient power generation with peak load shifting and CO_2 capture. *Energy* **2019**, *174*, 478–487. [CrossRef]